SCIA '97 The 10th Scandinavian Conference on Image Analysis
Lappeenranta, Finland, June 9-11, 1997

Modeling and Visualization for Pearl Quality Evaluation Simulator

Noriko Nagata, Teruo Usami
Industrial Electronics & Systems Laboratory,
Mitsubishi Electric Corporation,
8-1-1 Tsukaguchi-honmachi, Amagasaki, 661 Japan

Toshimasa Dobashi, Yoshitsugu Manabe and Seiji Inokuchi
Department of Systems Engineering,
Osaka University,
1-3 Machikaneyama-cho, Toyonaka, 560 Japan

Abstract

Visual simulation using CG and VR has attracted wide attention in machine vision. This paper proposes a method of modeling and visualizing pearls that will be the central technique of a pearl quality evaluation simulator. Pearls manifest a very specific optical phenomenon that is not dependent on the direction of the light source. To investigate this feature, we propose a physical model for multilayer film interference considering the multiple reflection in spherical bodies. The rendering algorithm has been configured from such representations of physical characteristics as interference, reflection and texture which correspond respectively to the sense of depth, brightness and grain that are the main evaluation factors obtained from psychological experiments. Further, portions of photos of real pearls and the images generated by the present method were evaluated based on a scale of psychological evaluation of " pearl-like quality" demonstrating thereby that not merely the generated images as a whole but the respective parts of images can present such a pearl-like quality.

1. Introduction

Visual simulation using computer graphics and virtual reality has come to be used recently in machine vision to enhance measurement and inspection systems. This approach is an analysis by synthesis method which is employed to find the optimum inspection conditions or inspection criteria through the simulation of the item for inspection. It is considered to be an important technology which will meet the needs to upgrade inspection systems and improving their accuracy.

In developing the pearl quality evaluation system, the authors have so far made various analytical approaches including factor analysis [1] and factor identification using neural networks [2], and succeeded in deriving a relationship between the physical information regarding pearls and their evaluation by human experts. We have this time studied a visual simulator which can form a virtual pearl sample in order to verify and correct the analytical results of the synthetic approach shown in Fig. 1.

Pearls (shown in Fig. 2) are widely known and remarkably popular as jewelry items. They also have the specific optical and structural features given below [3].

- A pearl has a unique and lustrous iridescence with its multilayer, thin-film structure, due to its diverse optical behavior such as refraction, interference and multiple reflection. Above all, the phenomenon of the hue distribution of the interference of light is characteristic. It constantly shows a concentric change from the center of the sphere without depending on the direction of the light source.
- A pearl is a natural substance whose film thickness and surface roughness are non-uniform indicating natural irregularities and fluctuations.

The modeling and visualization of a pearl, a substance interesting from the optical point of view as was seen above, is, therefore, a worthwhile topic for investigation.

Several studies have so far been made concerning the simulation of light behavior [4]. However little attention has been paid to multilayer, thin-film interference. Moreover, an investigation of the optical phenomenon of pearl mica paint has been reported [5], however, no such report has ever been made on the pearl.

The ultimate goal of this research is to clarify the inspection criteria by using various kinds of virtual samples, and collecting and analyzing the intuitive judgments of human experts. This paper proposes a pearl generating algorithm based on a physical model which will become the central technique for the planned simulator. In order to represent the specific

hue distribution independently of the direction of the light source, we propose a physical model for multilayer thin-film interference in a spherical body called an "illuminant model," that deals with each point in the layer as a point light source. Also, it was revealed in our previous study that psychological factors in the quality evaluation of pearls include a sense of depth, of brightness and of grain [1]. Therefore, the image generating algorithm is configured from such representations of physical characteristics as interference, reflection and texture, which correspond with these three psychological factors. Furthermore, in the process of image generation a psychological scale we call the " pearl-like quality" is configured from portions of photos of real pearls, which are then matched with " pearl-like quality" compositions of the corresponding portions of the generated images in order to evaluate them.

2. Modeling a Pearl

2.1 Physical Model of Multilayer Thin-Film Interference

A pearl is composed of a nucleus and nacreous layers surrounding it. The nacreous layers are formed of translucent films of 300 to 800 nm thick aragonite crystallized layers and less than 20 nm thick protein membranes alternatively deposited concentricity in 60 to 1000 stacks. When the highly transparent crystallized layers are laminated uniformly, a unique lustrous iridescence appears due to interference and multiple reflection [3]. This phenomenon is regarded as a multilayer thin-film interference caused by 2 kinds of optical film with different refractive indexes [6].

The particular characteristic of a pearl is the hue distribution of the interference color. Through the observation of a real pearl, we can see that the color appears on the opposite side to the light source where light does not hit directly, and also changes concentrically from the center of the sphere. In other words, the interference color of a pearl depends solely on the direction of the eyes, and not on the direction of the light source. In normal thin-film interference, the color change of the interference light source largely depends on the direction of the light source. This is because the phase difference of two interference waves depends on the incident angle of the light.

In order to simulate this phenomenon, we propose a physical model of multilayer thin-film interference called an " i lluminant model" which pays careful attention to the multiple reflection of light inside a pearl as shown in Fig. 3. Some of the light reaching the pearl surface goes inside the pearl, is repeatedly reflected and transmitted and is propagated to the rear of the nucleus before being distributed over the whole nacreous layer. As a result, it appears as if each point in the layer had a point light source transmitting rays in all directions, with each ray causing local interference as shown in Fig. 4. In other words, the light waves reflected on the boundary surfaces of each layer interfere with each other within the extremely short coherence distance of natural light. Here, as the phase difference of the reflected wave is determined by the angle between the reflected wave and the nacreous layer, the power spectrum of the interference light depends only on the refractive angle. As the interference takes place everywhere in the nacreous layer, each interference ray is propagated in all directions outside the pearl. Taking account of only the interference light waves propagated in the direction of viewpoints (a) and (b) in Fig. 3, the light from each point on the concentric circle is the interference light propagated with the same angle of refraction, so that the phase difference, i.e. the spectrum distribution must be equivalent. It follows from this that the independence of the interference light color from the direction of the light source and its change in concentric form can thus be explained.

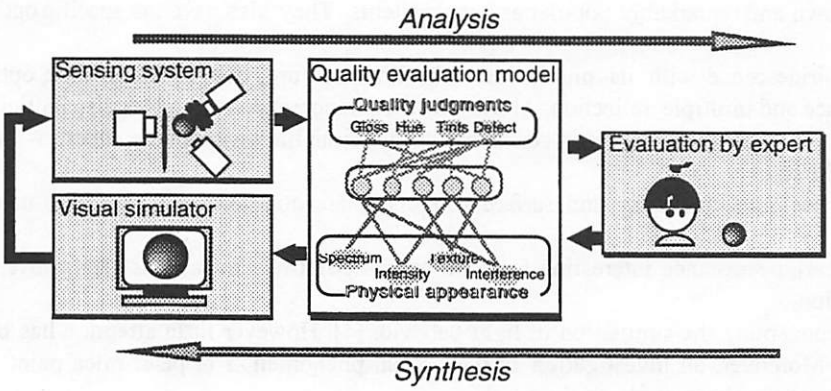

Fig. 1 Process of building up a pearl quality evaluation system by analytical and synthesis approach.

Fig. 2 Appearance of pearl.

2.2 Calculation algorithm of interference light

Figure 4 shows the structure of the nacreous layers and the behavior of the interference. The multilayer structure is composed of L layers, each alternately composed of stacks of crystallized nacreous layers of thickness d_l and of thin protein membranes. Here n_0, n_1, n_2 are the refractive indices of the air spaces, crystallized layers and protein membranes respectively.

The flow of the interference light calculation is as follows. First the crystallized layer film thickness column is generated, followed by casting a ray from the viewpoint to calculate the intersection with the pearl. The incident angle, reflectance and transmittance of all intersecting rays are calculated before making interference calculations from the outer layer to the inner layer of the nacreous layer for all visible wavelength bands in order to obtain the spectral power. The methods of calculation are given below.

2.2.1 Generation of crystallized layer film thickness column

As mentioned above, a pearl is a natural object, so that the structure of its layers is not uniform. The growth of a pearl corresponds to the changes in the season. Hence a film thickness generation method which imitates the growing process of a pearl can make it possible to evaluate or represent a natural pearl.

As a method of generating the crystallized layer thickness column d_l, the thickness (400-700 nm) per layer and the number of films (1-3) per day are expressed by the normal distribution functions, and the thickness and number of films are further varied by using random numbers. The parameters of these functions are determined by the growth curve of the pearl [3]. The thickness of the protein membrane is set to a constant 20 nm.

2.2.2 Calculation of incident angle

The interference light calculation is carried out only for light which reaches the viewpoint. The light arriving at the viewpoint from point P_0 on the pearl surface is considered as follows: first, a single ray in a nacreous layer is reflected by the l layer to the $l+m$ layer, and divided into the coherent rays i_l to i_{l+m}, which later interfere with each other. Next, the interference light enters at P_0 from the nacreous layer with a refractive index n_1 to the air space of refractive index n_0 at the angle of incidence θ_1, and refracts at the angle θ_0. Therefore, from the viewpoint and the position of point P_0, the visual angle or the refractive angle θ_0 is determined uniquely, and the angle of incidence θ_1 is calculated from Snell's law.

2.2.3 Calculation of reflectance/transmittance

The reflectance or transmittance is essentially determined by the refractive index of an object and the incident angle of light, and can be calculated using Fresnel's equations [6]. The reflectance to be considered here is the reflectance between the crystallized layer and the air space, and between the crystallized layer and the protein membrane.

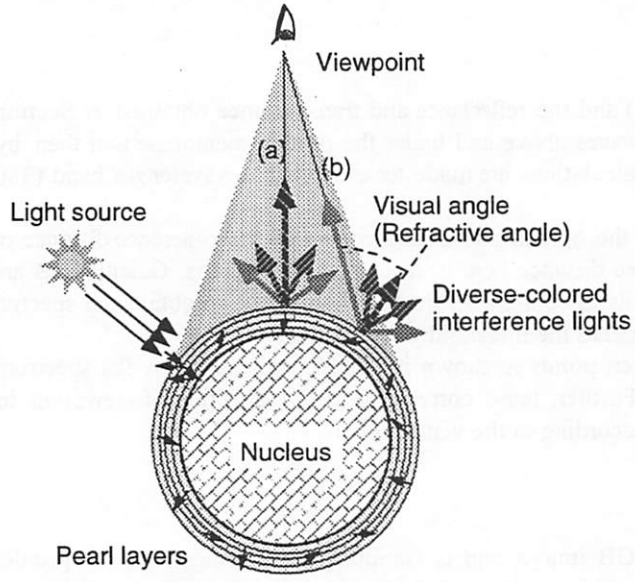

Fig. 3 Physical model of multilayer thin films of pearl.

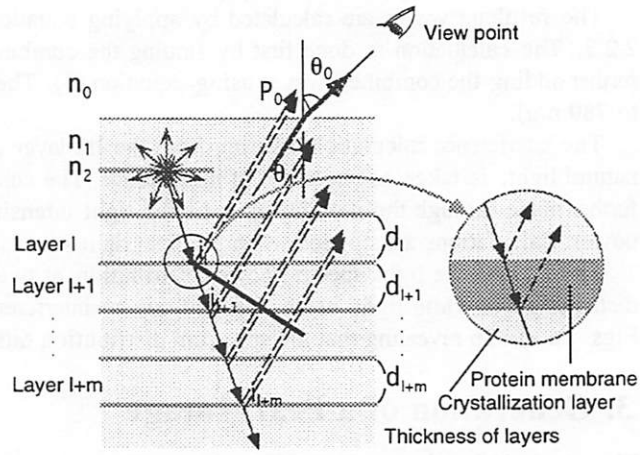

Fig. 4 Interference of incident light in nacreous layer.

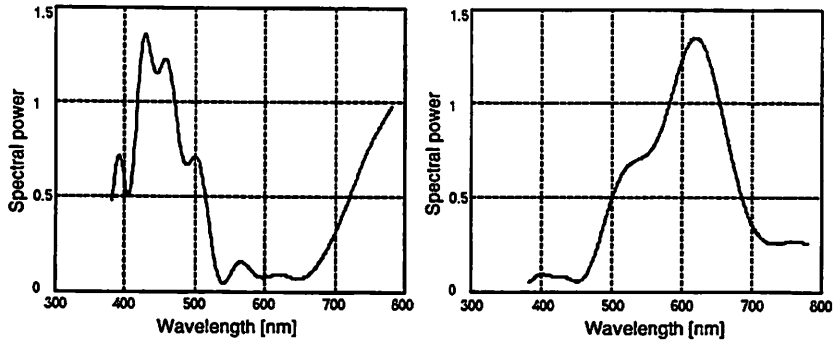

Fig. 5 Spectral power distribution of an interference light.

First, the energy reflectance R_1 ("reflectance") and the energy transmittance T_1 (" transmittance") when the light enters from the crystallized layer to the air space can be calculated by using Fresnel's equations in the following manner.

$$R_1 = \frac{1}{2}\left(|r_{\parallel}|^2 + |r_{\perp}|^2\right), \tag{1}$$

$$T_1 = 1 - R_1, \tag{2}$$

where: $r_{\parallel} = \dfrac{n_1 \cos\theta_0 - n_0 \cos\theta_1}{n_1 \cos\theta_0 + n_0 \cos\theta_1}$, $r_{\perp} = \dfrac{n_1 \cos\theta_1 - n_0 \cos\theta_0}{n_1 \cos\theta_1 + n_0 \cos\theta_0}$.

Here, $r_{\parallel}, r_{\perp}$ are the amplitude reflectances for p-polarized light and for s-polarized light respectively. Since these polarizations are contained equally in natural light, the values of R_1 and T_1 are obtained in the above manner. The refractive index n_1 is calculated by taking the C-axis refractive index of aragonite crystal as 1.53, and n_0 as 1.0.

Next, the reflectance R_2 and the transmittance T_2 between the crystallized layer and the protein membrane are also calculated in the same manner. Although the refractive index n_2 of the protein membrane is not known, it is regarded as 1.43.

2.2.4 Calculation of power spectrum

Thinking of the light transmitting from the outer to the inner layer with the incident angle calculated in Section 2.2.2., the reflected light waves are combined by calculating the phase differences between the waves. The phase difference due to the difference in the optical path between the reflected lights at the l layer and the $l+k$ layer is computable for the wavelength λ with the following formula.

$$\xi = 4\pi \sum_{i=l+1}^{k} d_i\left(n_1 / n_0\right) \cos\theta_1 / \lambda \tag{3}$$

The resultant waves are calculated by applying equation (3) and the reflectance and transmittance obtained in Section 2.2.3. The calculation is done first by finding the combined waves above and under the protein membrane and then by further adding the combined waves using equation (3). These calculations are made for each visible wavelength band (380 to 780 nm).

The interference calculation, starting from the 1st layer until the optical path difference reaches the coherence distance of natural light, is taken as one cycle of interference. The coherence distance here is regarded as 5 microns. Calculations are further made through the next layers until the light intensity fails to conform to the threshold value to obtain the spectral power. Calculations are stopped when the final light intensity reaches the threshold value of 0.05.

The interference light spectral power distribution at two given points is shown in Fig. 5, indicating the flat spectrum distribution of white light being changed due to interference. Further, these correspond to the direction of viewpoint in Figs. 3a and 3b revealing that the spectrum distribution differs according to the visual angle.

3. Generation of a Pearl Image

The obtained interference light spectrum is converted into a RGB image, and is combined with components of specular reflection and diffuse reflection to generate the pearl image. In order to evaluate the pearl quality in particular, the three major psychological factors: sense of depth (layer uniformity), sense of brightness (surface reflection) and sense of grain (surface uniformity), are given due weight.

3.1 Representation of the sense of depth due to interference light

The sense of depth corresponds to the expressions " thickly rolled," " strong tint," obtained through the questionnaires given to human experts, and is considered to be related mainly to the intensity of interference color [1]. The diffuse reflection as well as the film thickness and the number of films is considered to be the parameter likely to change the sense of depth, which is regarded as a function of diffusion in a normal rendering model. Hence, the sense of depth is expressed by calculating the diffuse reflected light by using the object color of the pearl, and then varying the mixing ratio with the interference light. Fig. 6a shows the image of the diffuse reflected light component. Fig. 6b shows an example of the image of the interference light component, where the bluish rainbow color, considered to be the most beautiful of the pearl interference lights, can be clearly observed.

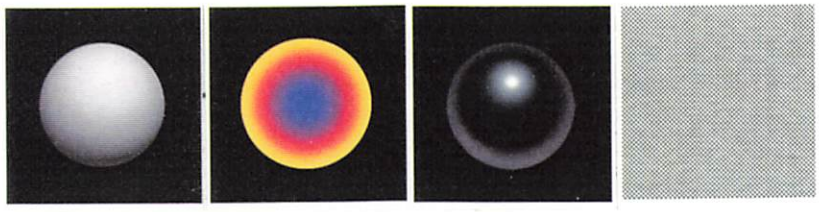

(a) (b) (c) (d)

Fig. 6 Components of a synthesized image.
(a) An diffuse image. (b) A Interference image. (c) A mirroring image. (d) Texture(V).

(a)	(b)	(c)
(d)	(e)	(f)
(g)	(h)	(i)

Fig. 7 Synthesized images.

Fig. 8 A synthesized image with texture.

Fig. 9 A synthesized pearl (left) and a real pearl (right).

3.2 Representation of the sense of brightness due to mirroring

Careful observation of a pearl shows that the background and the illumination of the circumference are mirrored well on the surface of the pearl. This was expressed by the experts during interviews as " mirroring one's face well [1]." In order to represent the difference in mirroring due to the surface properties of a pearl, the Torrance-Sparrow model [7] is used for the light source, and the surface properties are expressed by varying the microscopic surface distribution and the decrement coefficient parameters. The ray tracing method is used to mirror the surrounding object, and the optical decrement effect due to the distance between the nacreous surface and the object is also provided. An example of the image of the mirrored light source and the table is given in Fig. 6c.

3.3 Representation of the sense of grain due to texture

Unique textures expressed by " zara zara" (rough) or "mera mera" (flame like) are observed on the surface of a pearl. These textures are caused by the irregular striped patterns on the surface of a pearl. As a simple method of generating such textures, the high frequency component, extracted from the photograph of a real pearl by using two-dimensional FFT, band-passfilter and inverse FFT, is mapped on the nacreous surface. In order to enable an intuitive understanding and to allow the easy setting of parameters, the RGB of the image is converted into the Munsell color system (HVC space), and the texture factors of hue (H), value (V) and chroma (C) are used. The example of V texture (with expanded density scale) is shown in Fig. 6d.

3.4 Example of synthesis

The generated component images are synthesized as follows. The power spectrum of light is converted into a HVC image once, so that the mapping texture has an appropriate weight, before being converted into a RGB image. This time we used H and C factors for the diffuse reflection image, and V for the mirroring image, while adding the appropriate weight proportional to the V based on experience.

Examples of synthesis using this method are given in Fig. 7. The diffuse component, interference component and mirroring component are combined. The light source makes an angle of 45 degrees with the view direction, and the interference color is calculated independently of the direction of the light source. However, a contradiction is not felt, and a realistic pearl interference can be represented. A sense of brightness and transparency is also expressed by mirroring. By varying the mixing ratio of the interference image and the diffuse image, the difference in the sense of depth is shown. In Figs. 7a to 7i, the more to the left an image is the stronger is the sense of depth. By varying the parameters of the mirroring image, the difference in brightness is shown. The higher images are brighter. Fig. 8 shows the texture added to Fig. 7a. Slight as the color change is, it is confirmed by experts that the change improves the sense of grain and reality on the surface of the pearl.

To allow a comparison of our result with real pearls, the superimposition of the synthesized image on a photo of real pearls is shown in Fig. 9. It follows, therefore, that this method can effectively represent the optical phenomena of pearls.

4. Psychological Scaling of "Pearl-like Quality"

So far there is hardly any general method of making a quantitative evaluation of a CG expressed image. In this section we would like to try the evaluation of synthesized images by using the expression "-like quality."

The CG representation method can be broadly divided into two types--one is to bring the image infinitely close to the real object by using physical phenomenon and a mathematical model (Expression of reality), and the other is to make the object more real than itself by effectively extracting (and sometimes even by exaggerating) the modeling features and movements as in the case of deformation in a portrait (Expression of abstraction). In consideration of the various restrictions such as the characteristics of the display device, calculation cost, etc., the simulation of pearls can be carried out by making an abstract evaluation of the pearl features and by emphasizing the relevant factors, while utilizing a realistic expression based on a physical model, in order to bring the expression closer to the real thing.

Therefore, we closely examine this abstract-like quality. First, in order to learn what kind of spatial pattern a person senses in as a pearl, psychological experiments were carried out when generating the pearl images by using the key words pearl-like quality. The method of paired comparisons of Thurstone for nonexperts was used in carrying out a rating experiment to construct a psychological scale of pearl-like quality. Second, the synthesized images of a pearl are evaluated using the same method by means of the pearl-like quality scale, and then compared with the photographs.

4.1 Evaluation 1 Photo

Seven kinds of subregion with different characteristics were cut from an enlarged photograph of a pearl as shown in Fig. 10.

Next, 21 samples for evaluation, each consisting of two arbitrary subregions were made. A total of 103 university students were asked to make evaluations as to " which sample has the more pearl-like quality." For comparison, 2 rating cases were adopted: before and after observing a real pearl.

The psychological scale values due to the paired comparison method are shown in Fig. 11, with photographs 1 to 7 indicating the order from the center of a pearl. Further, the psychological scale values obtained after and before showing the real pearl to men and women are respectively shown in Fig. 12. The following results were obtained.

- The result on the whole shows it was felt that the most pearl-like photograph was the one containing both specular reflections and interference colors (Photo 2). It was followed by the photograph with interference colors only (Photo 4) and the photograph containing specular reflections only (Photo 1). The photographs including the profiles were given poor ratings for pearl-like quality (Photos 5,6,7).
- The distance of psychological scale values between the groups of pearl-like photographs (Photos 1,2,3,4) and non pearl-like photographs (Photos 5,6,7) was found to be larger, comparing the dispersion in the groups, for the case when real pearls were observed than when they were not. Similarly, women, normally more familiar with pearls, apparently have a wider psychological scale distance than men. These values, if regarded as the relative distance of dispersion, can evidently be taken as the scale for pearl-like quality.

These results thus indicate that a common psychological scale of pearl-like quality also exists among non-expert people. The sense of pearl-like quality depends on factors related to specular reflections and interference colors. It is

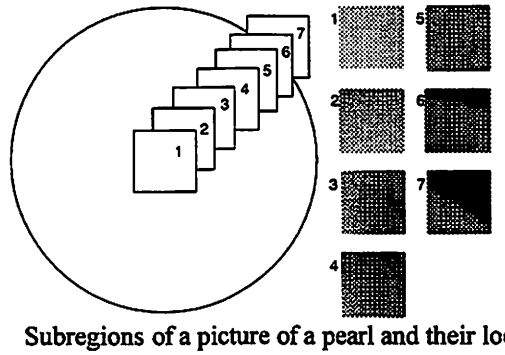

Fig. 10 Subregions of a picture of a pearl and their locations.

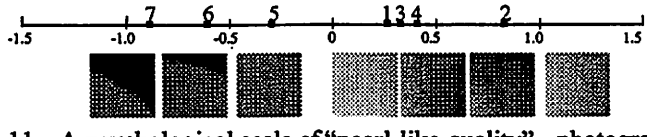

Fig. 11 A psychological scale of "pearl-like quality" - photograph -.

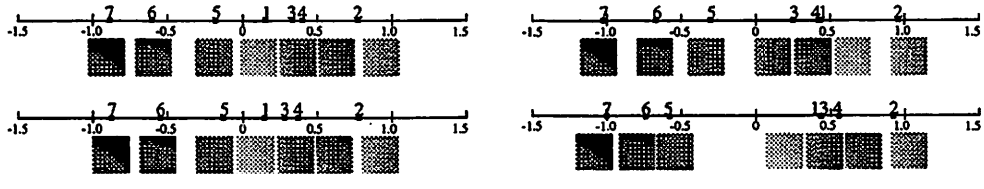

Fig. 12 Comparison of psychological scales.
(a) Before observing a real pearl. (b) After observing a real pearl.
(c) Men. (d) Women.

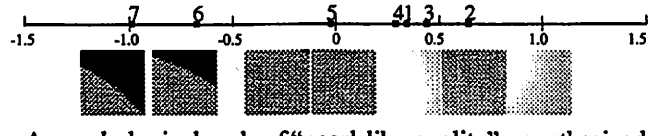

Fig. 13 A psychological scale of "pearl-like quality" - synthesized image -.

considered that this sense corresponds to " teri" and "maki," the technical terms implying the luster and interference color characteristic of a pearl, and a common sense of a pearl exists between experts and non-experts. It has also become clear that the profile of a pearl, i.e. the configurative factor is of little influence on the pearl-like quality.

4.2 Evaluation 2 synthesized image

Seven kinds of subregion were cut from the synthesized image in the same manner as in Fig. 10 as samples for evaluation. A total of 50 university students were asked to evaluate the samples on the basis of their pearl-like quality.

The psychological scale values are given in Fig. 13. As compared with the order of scale values obtained from the photographs, the order is the same except for image No. 4, which is 2 ranks down. No change in order is seen in the other samples, so that the synthesized images on the whole do give the features of the real pearl. The reason of the low ranking of image No. 4 seems to be that the smooth change in color in images No. 1 and No. 3 causes the evaluation of pearl-like quality to become relatively weak. Furthermore, image No. 2, evaluated as the most pearl-like, does not have its rank lowered, but has a poor evaluation. This is attributed to the conspicuous roughness of the image.

It can, therefore, be deduced that the synthesized images can give not only entire but also partial representations of pearl-like quality. Also the pearl-like quality involves smoothness, particularly the smoothness in color change.

5. Conclusion

We have proposed a representation technique for pearls on the basis of a physical model and a psychological evaluation in building up a visual simulator for pearls. This technique can be applied easily to clarify the inspection criteria of inspectors, which is the ultimate goal of our research. The parameters here are determined on the basis of experience, but the representation has been found to be more than satisfactory for multilayer thin-film interference which has so far not been tried in the field of CG.

By using a psychological scale of pearl-like quality we have next evaluated the photographs of a real pearl and synthesized images. The results show that a synthesized image can make a partial as well as a total simulation of the pearl-like quality. Furthermore, essential information has been acquired for representing real pearls. It is expected that the information can be used also in image generation to reduce the computing time by making a coarse calculation of factors not contributing to pearl-like quality.

However, the method needs further improvements from the standpoint of a photo-realistic representation of pearls. Some experts pointed out the lack of the sense of brightness in the synthesized images. In the representation of mirroring we would like to work on a physical model where the surface roughness and the spread or ooze of light are taken into account. As for textures, the introduction of chaos modeling, etc is also considered to represent the dynamic fluctuation.

In the future we plan to study the correspondence of the psychological and physical factors of the inspectors on the basis of this model. We also plan to select the physical parameters that could contribute to the pearl-like quality.

References

[1] K. Takamoto, M. Ito, A. Fukui, K. Takada and K. Nishii, Detection of micro cracks on ceramic devices, Proc. SICE Sensing Forum, no.12, pp.85-90, 1995.

[2] N. Nagata, M. Kamei, M. Akane and H. Nakajima, Development of a Pearl Quality Evaluation System Based on an Instrumentation of "Kansei", Trans. IEE Japan, vol.112-C, no.2, 1992.

[3] N. Nagata, M. Kamei and T. Usami, Transferring human sensibilities to machines - sensitivity analysis of layered neural networks and its application to pearl color evaluation -, Proc. MVA'94 IAPR Workshop on Machine Vision Applications, pp.528-531, 1994.

[4] K. Wada, Pearl. The national jewelry association, 1982.

[5] P. Poulin and A. Fournier, A Model for Anisotropic Reflection, Computer Graphics Proc., Ann. Conf. Series, vol. 24, no. 4, pp.273-282, 1990.

[6] P. Hanrahan and W. Krueger, Reflection from Layered Surfaces due to Subsurface Scattering, Computer Graphics Proc., Ann. Conf. Series, pp.213-220, 1994.

[7] J.S. Gondek, G.W. Meyer and J.G. Newman, Wavelength Dependent Reflectance Functions, Computer Graphics Proc., Ann. Conf. Series, pp.213-220, 1994.

[8] H.A. Macleod, Thin-Film Optical Filters. Techno House, 1986.

[9] K.E. Torrance and E.M. Sparrow, Theory for Off-Specular Reflection From Roughened Surfaces, J. the Optical Society of America, vol.54, no.91, pp.1105-1114, 1967.